Propionic acid-related inhibition during anaerobic digestion: insights into methane production and microbial community adaptation

Xiaojun Liu[1], Chloé Soulard[1, 2], Véronique Jamilloux[3], André Pauss[1], Laura André[4], Thierry Ribeiro[1], Sabrina Guérin-Rechdaoui[5], Vincent Rocher[5], Carlyne Lacroix[5], Chrystelle Bureau[3], Cédric Midoux[3-6-7], Olivier Chapleur[3], Ariane Bize[3], Céline Roose-Amsaleg[2]

1 Université de technologie de Compiègne, ESCOM, TIMR, Alliance Sorbonne Université, Compiègne, France

2 CNRS UMR 6553 Ecobio, Université Rennes 1, 35000, Rennes France

3 Université Paris-Saclay, INRAE, PROSE, 92761, Antony, France

4 Institut Polytechnique UniLaSalle, Université d'Artois, ULR 7519, Rue Pierre Waguet, BP 30313, CEDEX, 60026 Beauvais, France

5 SIAAP, Innovation department, 82 avenue Kléber, 92700 Colombes, France

6 Université Paris-Saclay, INRAE, MaIAGE, 78350, Jouy-en-Josas, France

7 Université Paris-Saclay, INRAE, BioinfOmics, MIGALE bioinformatics facility, 78350, Jouy-en-Josas, France

Corresponding author: ariane.bize@inrae.fr

Abstract

Propionic acid (HPr) accumulation is a major indicator of anaerobic digestion (AD) dysfunction, yet the relative contributions of acidity, undissociated HPr, and propionate ions (Pr^-) to process inhibition remain poorly understood. We investigated these effects in mesophilic batch AD microcosms fed with municipal sewage sludge, using a comparative design involving HPr, sodium propionate (NaPr), NaCl, and HCl treatments across two series of experiments. While 20 mM HPr caused a 22% reduction in the maximal methane production rate, 81 mM HPr led to complete inhibition, with the initial pH dropping to 5.1. By contrast, 81 mM NaPr reduced methane production rate by only 40%, and 81 mM NaCl caused no inhibition, demonstrating that acidity is the dominant inhibitory factor, with Pr^- exerting a secondary concentration-dependent effect. *16S rRNA* gene amplicon sequencing revealed strong, compound-specific shifts in microbial community composition, affecting key functional groups including syntrophs and methanogenic archaea. The proportion of methanogens dropped from 2-3% in control reactors to less than 0.2% under 81 mM HPr, consistent with the observed methane production inhibition. Under HPr81, over 100 ASVs were differentially abundant compared to controls, a pattern largely shared with HCl-treated reactors, further confirming the predominant role of acidity. The number of differentially abundant ASVs was negatively correlated with methane production rates (R^2 = 0.97), underscoring the link between community reshaping and process impairment. These results provide a unifying framework for propionate inhibition in AD and suggest that microbial community profiling could serve as an early warning tool for process imbalance detection.

Keywords: propionate; NaCl; pH; microbial community profiling; municipal sewage sludge; methanogenic archaea; syntrophy;

47 **1. Introduction**

48 Anaerobic digestion (AD) is an environmental biotechnology process for organic waste and
49 effluent treatment, that produces renewable energy (biogas), whose large-scale deployment
50 is a key target of European energy policy, highlighting the need to strongly understand and
51 optimize the AD process.

52 AD involves four microbial-mediated successive steps: hydrolysis, acidogenesis,
53 acetogenesis and methanogenesis. Acidogenesis converts long-chain fatty acids, amino
54 acids, and carbohydrates into volatile fatty acids (VFAs) like acetic, propionic (HPr), and
55 butyric acids. These VFAs may subsequently be consumed by acetogenic microorganisms
56 producing acetic acid, H_2 and CO_2, which are the main precursors for methane synthesis.
57 However, VFAs are also major inhibitors of AD, potentially leading to AD failure, as they
58 can accumulate due to an imbalance between acid production and consumption mediated by
59 acidogenic and acetogenic bacteria (reviewed in (Alavi-Borazjani et al., 2020)).

60 HPr (pK_a = 4.88) content is considered as an indicator predicting the dysfunction of AD
61 since it can accumulate in case of process dysfunction and is also toxic to the microbial
62 activities. During AD, HPr is rapidly dissociated into propionate (Pr^-) ions upon exposure to
63 AD medium, usually basic. When accumulating in important amounts, HPr, along with other
64 VFAs, can be responsible for the acidification of digesters by decreasing the pH (Sawyer et
65 al., 1954). Undissociated HPr, a form favored by lower extracellular pH (acidified
66 condition), penetrates the intracellular medium and dissociates there. The dissociation causes
67 a decrease in intracellular pH. To remediate this and maintain the proton gradient necessary
68 for ATP formation, the cell actively transports protons to the extracellular medium, thereby
69 reducing the ATP available for its growth and metabolism (Jiang et al., 2018). The
70 intracellular accumulation of dissociated HPr is also toxic to microorganisms, as it increases
71 intercellular ionic strength (Roe Andrew et al., 1998).

72 The inhibition of AD related to HPr has been studied for a variety of organic waste.

73 Nevertheless, the conclusions are very variable according to the study. Several works
74 observed no inhibition with HPr concentration up to 50 mM (equivalent to 3700 mg L^{-1})
75 during AD of diverse waste under both thermophilic and mesophilic conditions (Qiao et al.,
76 2013; Yang et al., 2015). In contrast, other studies (Demirel & Yenigün, 2002; Wang et al.,
77 2009) reported a decrease in biogas yield at HPr concentrations below 12.2 mM (903 mg L^{-}
78 ^{1}). Han and colleagues (Han et al., 2020) concluded that reversible inhibition with an
79 increased lag phase could occur at HPr concentrations above 22.7 mM (1,680 mg L^{-1}). This
80 variability is likely due to differences in the nature of the substrate and inoculum, as well as
81 other operating conditions. Moreover, HPr (Demirel & Yenigün, 2002; Wang et al., 2009)
82 or sodium propionate (NaPr, a weak base) (Yang et al., 2015) were used, with obvious
83 different effects. This highlights the need for further research to better disentangle the effects
84 of these different parameters through comparative analysis.
85 Understanding the microbial community response to increased HPr concentrations during
86 AD is moreover of interest to determine the extent, reproducibility and limits of microbial
87 community adaptation, but investigations have been limited to date. During AD, propionate
88 is converted by propionate oxidizers, particularly syntrophic propionate oxidizing bacteria
89 (SPOB) interacting with acetogenic and hydrogenotrophic methanogens (reviewed in
90 (Westerholm et al., 2022)). These two functional groups are likely to be affected by the
91 presence of HPr and are also known to be more sensitive to perturbations compared to
92 hydrolytic and acidogenic bacteria (Sikora et al., 2017). According to previous studies, a
93 shift from acetoclastic to hydrogenotrophic methanogenesis enabled the recovery of a
94 digester inhibited by HPr (Han et al., 2020). By contrast, Li and colleagues suggested the
95 positive role of *Methanotrichaceae*, which comprises exclusively acetoclastic methanogens,
96 during propionate degradation in the presence of high ammonia concentrations (Li et al.,
97 2017). This emphasizes the specificity of the microbial response to given operating
98 parameters. A recent study demonstrated that long-term exposure to extreme propionate

concentrations (up to 250 mM, i.e. 24 g L^{-1}) in mesophilic anaerobic co-digestion of chicken litter and sodium propionate (NaPr) led to the development of a functionally redundant microbiome capable of sustaining methane production; a shift in archaeal populations at around 62.5 mM (i.e. 6 g L^{-1} of NaPr), in particular from *Methanolinea* to *Methanoculleus*, both hydrogenotrophs, was observed (Ochoa-Bernal et al., 2025).

The present study is specifically focused on municipal sewage sludge (MSS) digestion, which is one of the major waste resources feeding anaerobic digesters (Scarlat et al., 2018). In 2023, 1.1 million tons (Mt) of dry matter (DM) MSS were produced in France and 1.6 in Germany, requiring effective valorization methods (EUROSTAT). To reach a unifying view on inhibition by HPr, the following questions are tackled. How does the presence of HPr affect the physico-chemical dynamics of AD as a function of its concentration? Is the observed inhibition primarily due to the presence of dissociated propionate or to the drop in pH caused by HPr dissociation? Finally, to what extent do microbial communities adapt to the presence of propionate and is this adaptation specific to the form in which propionate is added?

To address these issues, two series of tests in model systems, namely in mesophilic AD batch microcosms, were conducted according to an original experimental design. This study demonstrates that propionate itself exerts an inhibitory effect, albeit less pronounced than that of acidity, and highlights a gradual and substantial adaptation of microbial communities, which is nevertheless insufficient to completely offset the inhibition, and which is highly specific to the added compound.

2. Material and methods

2.1 Experimental study on propionic acid inhibition

2.1.1 Origin of inocula and substrates

All incubation experiments were conducted in AD microcosms. The substrate was a mixture

125 of primary, biological, and tertiary MSS collected from the Seine-Aval WWTP, which
126 processes 1 500 000 m^3 per day and serves the Paris conurbation (France). Digested sludge
127 used as inoculum was obtained from one of the mesophilic digesters at the same WWTP.
128 Different batches of both types of sludge were utilized for each test series, consistently
129 sourced from the same sampling points. The total solid content (TS), volatile solid content
130 (VS), and pH of the substrate ranged from 3.3% to 4.7% of fresh mass, 71% to 77% of TS
131 and 6.0 to 6.3, respectively; for the inoculum, these values were 2.3% to 2.6%, 61% to 63%
132 of TS, and 7.4 to 7.6, respectively (Supplementary file 1).
133

134 **2.1.2 Anaerobic digestion tests and reactor sampling**

135 Two series of Biochemical Methane Potential (BMP) tests were conducted and involved
136 different treatments (Table 1). The incubations were conducted using the AMPTS II
137 (Automatic Methane Potential Test System II, Bioprocess, Lund, Sweden), under batch and
138 mesophilic (37°C) conditions, following the guidelines of (Holliger et al., 2016).
139 In the first tests, the reactors contained 100 mL substrate (fresh MSS), 100 mL inoculum
140 (digested MSS), and 200 mL deionized water. HPr was added at 0, 13, 20, or 81 mM. To
141 analyze microbial communities and chemical parameters during the course of AD, two
142 reactors from each treatment were sacrificed on days 2, 4, 7, and 13, to collect their content,
143 except for treatment HPr13 that was not analyzed on day 13.
144 For the second tests, the operation lasted 22 days. Except for the controls without substrate
145 (Neg, 6 replicates) that contained the inoculum (200 mL) and deionized water (200 mL), all
146 other reactors were filled with both inoculum (200 mL) and substrate (200 mL). Either no
147 additional compound was added (Ctrl), or one among HPr, NaPr, NaCl and HCl (Table 1).
148 Regarding HCl, a 10% HCl solution was added dropwise to adjust the initial pH to 5.1, which
149 was the lowest initial pH observed experimentally, under HPr81 (Supplementary File 2,
150 Figure S1). The liquid phase was sampled for microbial community and chemical analysis

151 exclusively before incubation and at the final time point.

152

153 **Table 1. Experimental design for the first and second tests**

154

Name	Condition tested in 500-mL reactors	# BMP tests	Sampling times (days)	# 16S metabarcoding analyses[a]
First tests				
Ctrl	control (inoculum + MSS)	x 8	2, 4, 7, 13	9
HPr13	inoculum + MSS + 13 mmol L^{-1} HPr	x 6	2, 4, 7	7
HPr20	inoculum + MSS + 20 mmol L^{-1} HPr	x 8	2, 4, 7, 13	9
HPr81	inoculum + MSS + 81 mmol L^{-1} HPr	x 8	2, 4, 7, 13	9
Second tests				
Neg	negative control (inoculum only)	× 6	0, 22	6
Ctrl	positive control (inoculum + MSS)	× 5	0, 22	5
HPr20	inoculum + MSS + 20 mmol L^{-1} HPr	× 3	0, 22	3
NaPr20	inoculum + MSS + 20 mmol L^{-1} NaPr	× 3	0, 22	3
HPr81	inoculum + MSS + 81 mmol L^{-1} HPr	× 3	0, 22	3
NaPr81	inoculum + MSS + 81 mmol L^{-1} NaPr	× 3	0, 22	3
HCl	inoculum + MSS at pH = 5.1	× 3	0, 22	3
NaCl81	inoculum + MSS + 81 mmol L^{-1} NaCl	× 3	0, 22	3

155
156 [a] In addition to the reactor samples, the MSS and the inoculum were also analyzed by 16S rDNA metabarcoding
157

158 For both tests and at each sampling, 1.7 mL aliquots of the liquid phase were centrifuged at
159 10,000 g for 5 minutes. The pellets and supernatants were stored separately at -20°C until
160 subsequent DNA extraction and total VFA analysis (Supplementary File 3), respectively.
161 The pH values were determined on the fresh liquid phase samples, immediately after
162 collection, using a pH meter (Mettler Toledo, Switzerland).

163

164 **2.1.3 Curve modeling by modified Gompertz equation**

165 AMPTS recorded daily methane production for each reactor. The data were processed using
166 Office Excel 2019 (Microsoft®, Redmond, US). The modified Gompertz equation
167 (**Equation 1**) was used to estimate the kinetic parameters related to methane production for
168 each treatment, namely the biomethane potential and maximum production rate, as well as

169 the lag time. This thereby enabled the quantification and comparison of the possible
170 inhibition among different conditions. Non-linear regression for kinetic modeling was
171 performed using Scilab software (Dassault Systèmes, Vélizy-Villacoublay, France). The
172 model's goodness-of-fit was evaluated based on adjusted R^2, sum of squared errors, root
173 mean squared errors and mean absolute percentage error.

174 $$BMP(t) = BMP_0 / \{ 1 + \exp [R_m \cdot e \cdot (\lambda - t) / BMP_0 + 1] \}$$ (**Equation 1**)

175 where BMP(t) is the cumulative methane production at time t ($NL_{CH4} \cdot kg_{VS}^{-1}$ at 0°C, 1 atm),
176 BMP_0 is the maximum methane yield of the substrate tested ($NL_{CH4} \cdot kg_{VS}^{-1}$), R_m is the
177 maximum methane production rate ($NL_{CH4} \cdot kg_{VS}^{-1} . d^{-1}$), λ is the lag time (d), t is the
178 incubation duration (d) and e ≈ 2.7182.

179 ANOVA followed by a post hoc Tukey test were performed using R Studio (R Studio Inc.,
180 Massachusetts, USA) to assess significant differences between experimental results.

181

182 **2.2 Microbial community analysis**

183 **2.2.1 DNA extraction**

184 DNA extraction was conducted from the frozen pellets using the kit Nucleobond® RNA Soil
185 with the complementary DNA Set, following the manufacturer's instructions (Macherey-
186 Nagel, Düren, Germany). Mechanical cell lysis was performed with TissueLyser II (Qiagen,
187 Hilden, Germany). DNA concentrations were measured using Quantifluo with a SAFAS
188 spectrophotometer, employing the fluorescent dye Picogreen® (ThermoFisher, Waltham,
189 US).

190

191 **2.2.2 *16S rRNA* gene amplicon sequencing**

192 Sequencing of *16S rDNA* amplicons was performed using an Ion torrent PGM instrument
193 (Life Technologies, Carlsbad, US) after PCR amplification of the V4-V5 hypervariable
194 regions with the fusion primers 515F (5'-Ion A adapter - Barcode –

195 GTGYCAGCMGCCGCGGTA- 3') and 928R (5'- Ion trP1 adapter –
196 ACTYAAAKGAATTGRCGGGG-3'), as previously described (Poirier et al., 2016).
197 A total of 36 samples were processed for the first tests, and 29 samples for the second tests.
198 Raw reads were submitted to the ENA under project accession PRJEB87704.
199

200 **2.2.3 Bioinformatic processing**

201 Raw amplicon sequencing data were pre-processed with deepomics16S pipeline
202 (https://forge.inrae.fr/deepomics/deepomics16S v14.10.2022) on the servers of the INRAE
203 MIGALE bioinformatics platform. This pipeline employs DADA2 (Callahan et al., 2016),
204 for the generation of Amplicon Sequencing Variants (ASVs) and FROGS (Bernard et al.,
205 2021) for the taxonomic affiliation of ASVs, relying on Silva database
206 (silva_138.1_16S_pintail100). Only the V4 region was considered for samples of the second
207 tests due to a lower sequence quality, using primer sequences 5'-
208 GTGYCAGCMGCCGCGGTA and 5'-GGACTACHVGGGTWTCTAAT for trimming.
209 Each sample retained more than 15,000 sequences after bioinformatics processing
210 (Supplementary File 2, Figure S2). The raw sequences, biom files and physicochemical data
211 were deposited in a FAIR mode in DeepOmics information system (https://deepomics-
212 info.hub.inrae.fr/).
213

214 **2.2.4 Biostatistics analysis**

215 The pre-processed sequencing data were analyzed using R version 4.3.2 (Team, 2021) in
216 RStudio (2024.04.2+ 764) environment. Several specific packages were utilized, such as
217 ComDim 0.9.51 (https://github.com/f-puig/R.ComDim) for Common Component Analysis
218 (CCA), DESeq2 1.42.0 (Love et al., 2014) for differential abundance analysis and phyloseq
219 1.46.0 (McMurdie & Holmes, 2013) for barplot representation. The taxonomic tree was built
220 with GraPhlAn (https://github.com/biobakery/graphlan).

221 For the first tests, 157 Amplicon Sequence Variants (ASVs) were selected, by removing the
222 ASVs with less than 400 reads in the dataset. For the second tests, ASVs representing less
223 than 0.5% of the reads in the dataset were removed, resulting in 169 ASVs for analysis.
224 However, for the differential analysis, data from the second tests were filtered less strictly,
225 removing ASVs representing less than 400 reads, resulting in a total of 276 ASVs.
226

227 **3. Results**

228 **3.1 Inhibition of methane production increases with propionic acid (HPr)**
229 **concentration**

230 To decipher AD inhibition by HPr, four distinct concentrations of HPr: 0, 13, 20 and 81 mM,
231 were added to batch AD microcosms (first tests of this study, Table 1), aiming to obtain
232 contrasted inhibition levels. Based on cumulative methane production, inhibition increased
233 gradually with HPr concentration, reaching complete inhibition under HPr81 (Figure 1A).
234 Additionally, the pH values overall decreased with increasing HPr concentration, which can
235 be explained by both the dissociation of the added HPr and the accumulation of various
236 volatile fatty acids due to acidic inhibition of the process (Supplementary File 2, Figure S3).
237 Indeed, under HPr81, the pH values remained at 5 or 5.1 throughout the entire incubation
238 period (Supplementary File 2, Figure S1). Such pH values are known to inhibit the AD
239 process, especially methanogenesis (Clark & Speece, 1971).
240

241 **3.2 Methane production is more sensitive to acidic pH and propionic acid (HPr) than**
242 **to propionate ion (Pr^-)**

243 The negative effect on methane production following HPr addition may be attributed to the
244 propionic acid itself, its ionized form (propionate, Pr^-) and/or the low pH condition caused
245 by HPr dissociation, generating protons (H^+). To investigate different possible effects,
246 distinct incubation conditions were established in second AD tests, by varying the nature of

247 the counterions or targeting specific pH values (Materials and methods, Table 1). Pairwise
248 comparisons between the treatments enabled investigation of the specific effects of certain
249 ions. Comparison of HPr20 and NaPr20 on the one hand, HPr81 and NaPr81 on the other,
250 enabled to assess the contribution of acidity to the observed effects. In addition, NaCl81
251 treatment aimed to verify the absence of inhibition by sodium ions. Finally, HCl was added
252 to obtain an initial pH value of 5.1, the same as that measured under HPr81, to assess the
253 effect of a pH decrease that was not caused by the addition of HPr. Besides, treatments HPr20
254 and HPr81 also enabled comparison with the first tests.
255 The cumulative methane production of MSS under the different conditions was calculated
256 by subtracting the mean gas production obtained under Neg from the raw methane
257 productions (Figure 1B). The negative controls yielded 56 ± 2 NL_{CH4} kg_{VS}^{-1}, which meets
258 the acceptance criteria for BMP validity (Holliger et al., 2016). Ctrl yielded 250 $NL_{CH4}.kg_{VS}^{-}$
259 ^{1}, with no significant difference compared to production under NaCl81 (253 $NL_{CH4}.kg_{VS}^{-1}$).
260 This indicates that the concentrations of Na^{+} and Cl^{-} ions tested ($[Na^{+}] = [Cl^{-}] = 81$ mM) did
261 not inhibit the AD process. By contrast, under HPr81 or HCl, both leading to an acidic pH
262 of 5.1, no methane was produced.
263 The addition of propionate at lower levels, either in its HPr or NaPr form, contributed to a
264 delay in methane production, as indicated by the longer lag phases (λ) compared to Ctrl
265 (Table 2). However, it ultimately improved the methane yield (Table 2), which increased up
266 to 348 ± 5 $NL_{CH4}.kg_{VS}^{-1}$ for NaPr81. With the addition of HPr or NaPr, methane was
267 produced not only through MSS degradation, but also by the consumption of HPr or Pr^{-},
268 which acted as additional substrates for the microorganisms.
269

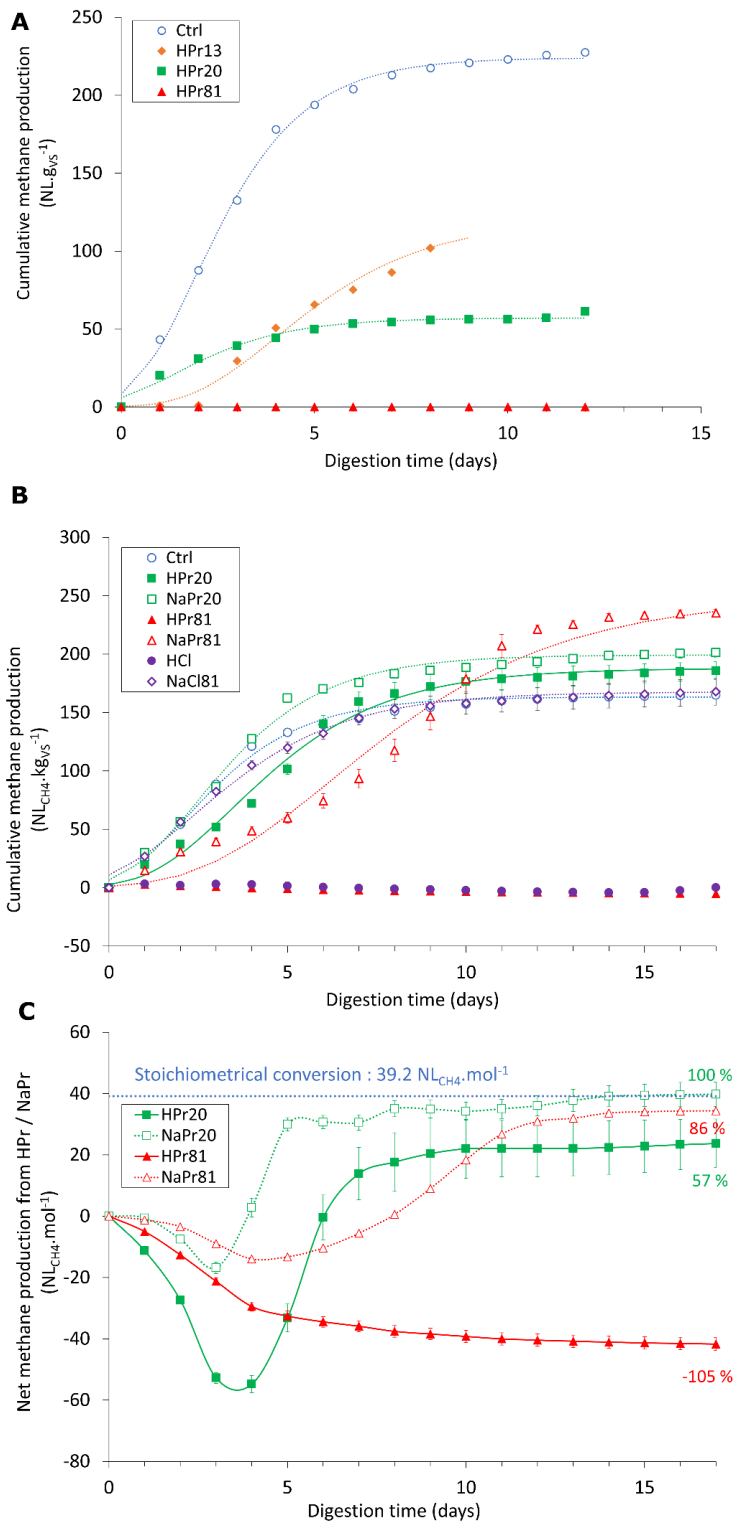

Figure 1. Methane production dynamics during the AD incubations

A. During the first tests. B. During the second tests. C. Net methane production over time during the second tests, obtained by subtracting methane production under Ctrl to the methane production under the considered conditions The curves are the averages of the replicates, the dotted lines are the results of Gompertz identifications (Equation 1).

The methane production under Ctrl was subtracted from that of the other treatments and compared to the stoichiometric production of methane from propionate and propionic acid, which is 39.2 NL_{CH4} mol^{-1} according to **Equation 2**:

$$CH_3CH_2COOH + 0.5\ H_2O \rightarrow 1.75\ CH_4 + 1.25\ CO_2 \qquad \textbf{(Equation 2)}$$

In Figure 1C, the comparison of NaPr and HPr treatments at the same molar concentrations highlighted the significant effect of pH and/or the undissociated form of HPr, compared to that of Pr^- ion. Methane was produced even for high Pr- concentration, despite a transient inhibition during the initial hours of the tests. The production reached almost 86% of the maximal methane production under NaPr81.

Overall, although the effect of HPr or the counterion H+ appears to be largely dominant in the inhibition phenomenon, a decrease in methane production rate was observed in the presence of high NaPr concentrations, highlighting the inhibitory effect of Pr- itself.

Table 2. Kinetic parameters of the modified Gompertz equation and fitting goodness for the second tests

Treatment assessed	BMP_0 (NL CH_4·kg VS^{-1})	λ (day)	R_m (NL CH_4·kg VS^{-1}·d^{-1})	MAPE* (%)	R^2 (–)
Ctrl	250 ± 2	0.35 ± 0.08	56.1 ± 3.9	2.16 ± 0.23	0.995 ± 0.002
HPr20	280 ± 14	1.13 ± 0.07	43.8 ± 2.9	8.70 ± 0.66	0.991 ± 0.001
NaPr20	291 ± 5	0.55 ± 0.01	57.8 ± 0.8	3.59 ± 0.14	0.995 ± 0.000
HPr81	NA**	NA	NA	NA	NA
NaPr81	348 ± 5	2.45 ± 0.22	33.7 ± 1.2	15.2 ± 1.0	0.981 ± 0.001
HCl	NA	NA	NA	NA	NA
NaCl81	253 ± 16	0.13 ± 0.03	43.4 ± 1.0	1.69 ± 0.14	0.996 ± 0.001

* Mean absolute percentage error of modeling
** Results are not available (NA) because the Gompertz equation was not suitable for the shape of curve
BMP0 is the maximum methane yield of the substrate tested, λ is the lag time and Rm is the maximum methane production rate

294

295 **3.3 Significant adaptation of microbial communities to propionic acid (HPr) occurs**
296 **during ecological successions, even with the smallest addition of HPr**

297 Since the effects on methane production are generally mediated by the response of the
298 catalytic microbial communities to the operating conditions, the adaptive dynamics of
299 microbial community composition was subsequently analyzed, through *16S rDNA*
300 metabarcoding.

301 Among the 16 bacterial phyla represented in the first tests, the six most abundant at day 13
302 were Bacteroidota, Spirochaetota Pseudomonadata, Bacillota, Chloroflexota, and
303 Candidatus Cloacimonadota (Supplementary File 2, Figure S4), all commonly identified in
304 anaerobic digesters (Calusinska et al., 2018; Jiang et al., 2021).

305 Archaea consistently represented less than 4% of the reads in the samples and predominantly
306 belonged to *Methanosarcina* and *Methanolinea* (Figure 2A). The first genus includes
307 metabolically-versatile methanogens encoding three methanogenesis pathways
308 (hydrogenotrophic, acetoclastic and methylotrophic) (Liu & Whitman, 2008), while the
309 second corresponds to strictly hydrogenotrophic methanogens (Sakai et al., 2012).

310

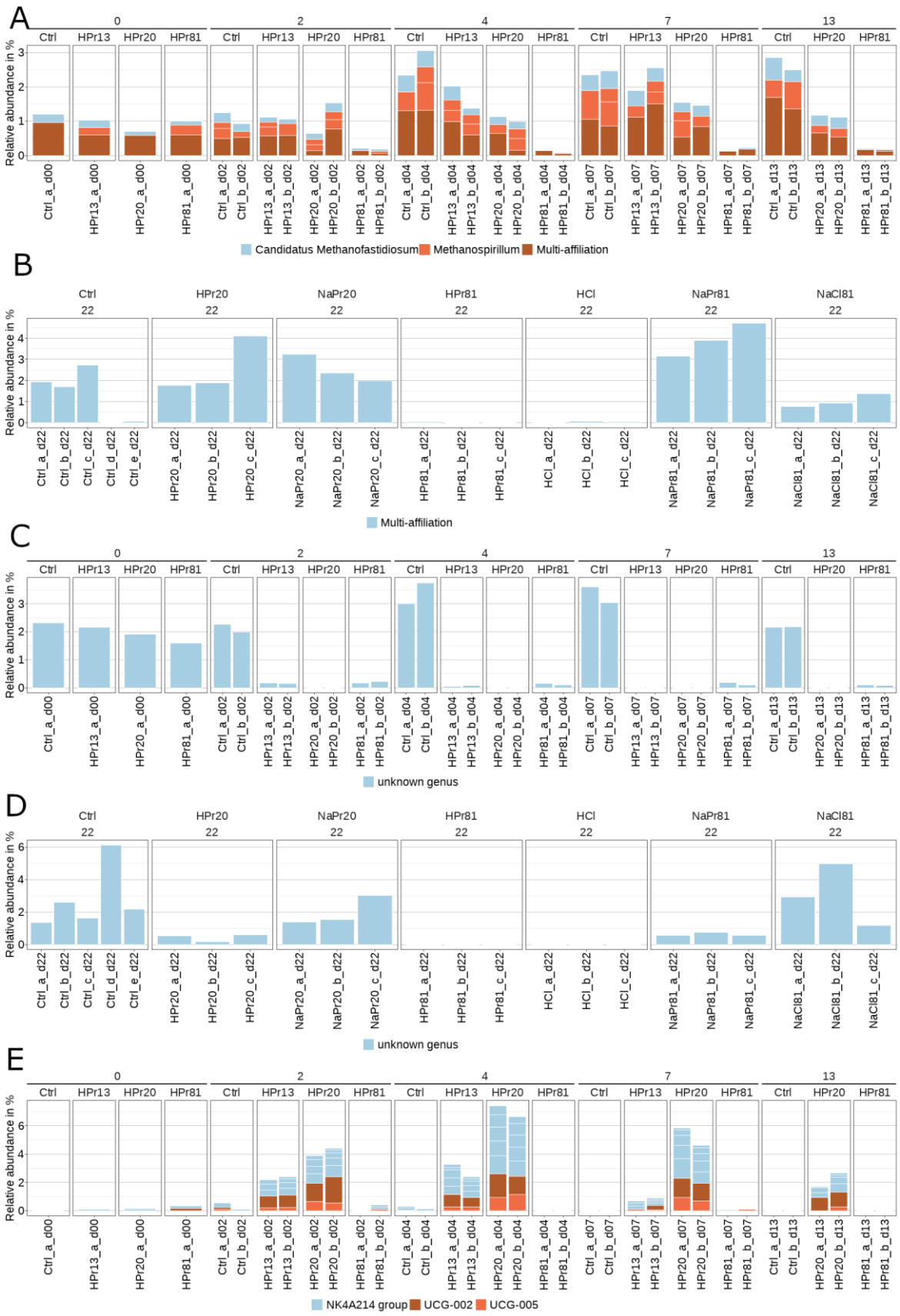
A
Relative abundance in %
Candidatus Methanofastidiosum
Methanospirillum
Multi-affiliation
B
Relative abundance in %
Multi-affiliation
C
Relative abundance in %
unknown genus
D
Relative abundance in %
unknown genus
E
Relative abundance in %
NK4A214 group
UCG-002
UCG-005

311

312

313

314 **Figure 2: Barplots of selected microbial groups of interest.** A. Relative abundance of
315 archaea in the first tests, at the genus level. B. Relative abundance of the archaea in the
316 second tests, at the genus level. C. Relative abundance of the family ST-12K33
317 (Sphingobacteriales order) in the first tests. D. Relative abundance of the family ST-12K33
318 (Sphingobacteriales order) in the second tests. E. Relative abundance of the family
319 Oscillospiraceae in the first tests. For the first and second tests, multi-affiliation corresponds
320 to *Methanothrix* and/or *Methanomicrobium*, most likely *Methanothrix.*
321
322
323 Based on PERMANOVA applied to the Bray-Curtis distance matrix of compositional data,
324 38% of the variance was explained by the addition of HPr and 24% by the incubation time
325 (`dist.bc ~ treatment * day of incubation`, 9999 permutations, p-value = 10^{-4} for both
326 factors). The dynamic adaptation of microbial communities to the presence of HPr was thus
327 clearly demonstrated.
328 A pronounced decrease in the proportion of reads attributed to archaea as a function of the
329 applied HPr concentration was observed (Figure 2A). At the end of the experiment (day 13),
330 this proportion reached nearly 3% in control reactors, between 1% and 2% in reactors with
331 intermediate HPr concentrations, and less than 0.2% in reactors exposed to the highest HPr
332 concentrations.
333
334 **3.4 HPr differentially affects over time a high number of microbial groups with**
335 **diverse functions**
336 To highlight microbial community patterns more thoroughly, a Common Component
337 Analysis (CCA) was conducted. This methods groups variables by their shared effects on
338 data dispersion, optimally weighting each variable's contribution (Jouan-Rimbaud
339 Bouveresse & Rutledge, 2024; Puig-Castellví et al., 2020). To extract relevant information

340 from CCA, different visualizations were cross-referenced. For each common component
341 (CC), Figure 3A illustrates the average scores of each treatment over time, revealing distinct
342 longitudinal profiles occurring in the various treatments. Figure 3B presents a taxonomic
343 tree of 75 distinct ASVs underlying these patterns (see also Supplementary File 2, Figure S5
344 and Supplementary File 4. Finally, the temporal evolution of these 75 ASVs was examined
345 individually through relative abundance barplots (Supplementary File 5, Figures S6-S91),
346 with Figure 3C illustrating an abundant ASV associated with CC1, assigned to the family
347 Anaerolineaceae.
348

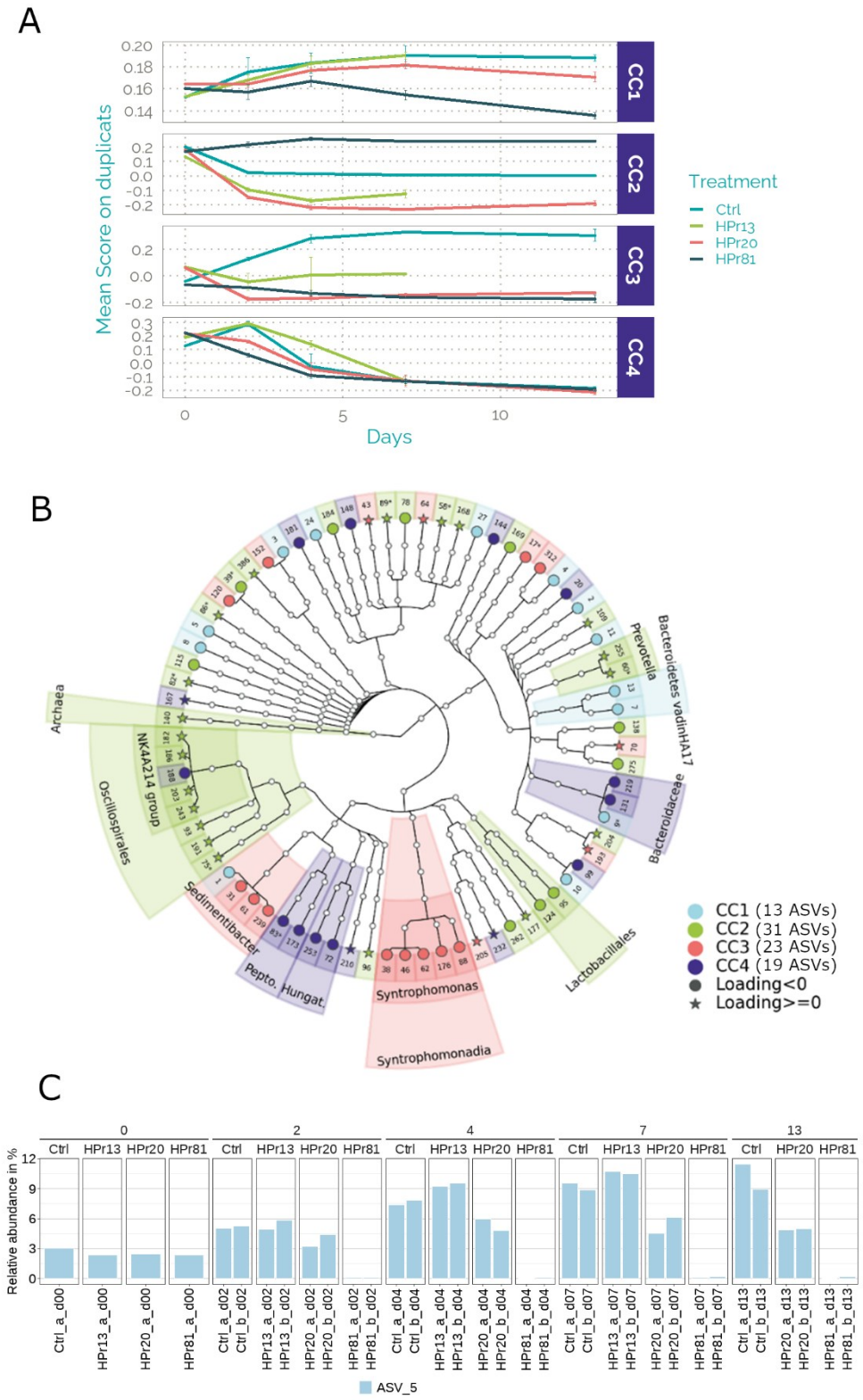

Figure 3. Illustration of Common Component Analysis (CCA) results for the first tests. A. Profiles over time of the AD reactors for the 4 first Common Components (CC); the average and standard deviation are shown, 2 replicates. B. Taxonomic tree of the ASVs contributing the most to the four first CCs. These ASVs were selected based on their

354 loadings, exceeding 1.5 times the standard deviation of all ASVs (Supplementary File 2,
355 Figure S5). C. Example of an ASV associated to CC1 (ASV_5: Bacteria, Chloroflexi,
356 Anaerolineae, Anaerolineales, Anaerolineaceae, unknown genus).
357
358
359 Clear and distinct trends of microbial community dynamics were observed across the four
360 CCs (Figure 3A). CC1 exhibited a particular trend for the highest HPr concentration
361 (HPr81), noticeable from day 4 and intensifying progressively over time. CC2 discriminated
362 high (HPr81), intermediate (HPr20), and low (HPr13 and Ctrl) HPr concentrations. CC3
363 revealed distinct evolutions between Ctrl and other treatment groups. Finally, CC4 exhibited
364 consistent trends among the different treatments, primarily reflecting temporal evolutions:
365 such ecological successions are anticipated due to progressive substrate depletion and
366 bioconversion under batch operating conditions.
367 In more detail, the 13 underlying ASVs identified for CC1, representing 12 families and 6
368 phyla, were among the most abundant, with most exceeding 5% relative abundance in at
369 least one sample. Four ASVs—assigned to Anaerolineaceae, Sedimentibacteraceae,
370 Dysgonomonadaceae, and Bacteroidetes vadinHA17—were strongly impaired under high
371 HPr exposure (HPr81), with ASV_1 (*Sedimentibacter*) being particularly sensitive even to
372 minimal HPr additions. In contrast, three ASVs—from Candidatus Cloacimonadaceae,
373 Tannerellaceae, and Lysobacteraceae—were selected under HPr81. Based on MIDAS
374 database (Dueholm et al., 2024), these 13 ASVs were predominantly acidogens, consistent
375 with the abundance of fermentable molecules in wastewater sludge.
376 The 31 ASVs associated to CC2 were distributed over 22 families, mostly from the phyla
377 Firmicutes, Bacteroidota and Proteobacteria. Corresponding to subdominant taxa, they
378 encompassed a wide range of functional groups. Notably, important shifts in fermenter
379 populations were observed with increasing HPr concentrations: six ASVs assigned to

380 Oscillospiraceae (Gophna et al., 2017) were selected under low to intermediate HPr
381 concentrations, while ASV_60 (*Prevotella*) and ASV_95 (*Lactobacillus*) were favored
382 under HPr81, reaching more than 6% and 3% of the reads, respectively. Besides, three ASVs
383 revealed highly sensitive to HPr, namely, ASV_140 (*Methanospirillum*), ASV_39
384 (*Smithella*) and ASV_17 (Sphingobacteriales, ST-12K33).
385 CC3 corresponded to subdominant taxa, with 13 out of 23 ASVs more abundant under Ctrl.
386 Eleven of these, including *Sedimentibacter* and *Syntrophomonas* members, were highly
387 sensitive to HPr. *Sedimentibacter* presumably corresponded to protein fermenters (Imachi et
388 al., 2016). *Syntrophomonas* bacteria oxidize butyrate or saturated fatty acids, producing
389 acetate and H_2, and, in some cases, propionate, depending on the substrate (Sekiguchi, 2015).
390 Consequently, they can develop syntrophic interactions with hydrogenotrophic methanogens
391 (Sousa et al., 2007). The remaining 10 underlying ASVs displayed various patterns
392 depending on HPr concentration: some reached peak abundance at intermediate HPr
393 concentrations (from families Tannerellaceae, Butyricicoccaceae) while others were more
394 abundant under the highest HPr concentration (from families Veillonellaceae and
395 Paludibacteraceae).
396 Overall, CCA confirmed that exposure to HPr affected the abundance of numerous ASVs
397 across diverse functional and phylogenetic groups, leading to several major shifts in
398 microbial composition as the initial HPr concentration increased.
399

400 **3.5 Each added compound affects specifically the microbial community composition**

401 To determine the extent to which the adaptation of the microbial community was driven by
402 the specific compound added, and in particular by the nature of the counterion (e.g. H^+ or
403 Na^+), *16S rDNA* metabarcoding was applied to samples from the second tests, collected in
404 each reactor at the end of the experiment, after 22 days of incubation. Out of 18 different
405 bacterial phyla, the six dominant ones were Bacteroidota, Bacillota, Candidatus

406 Cloacimonadota, Pseudomonadata, Chloroflexota, and Synergistota (Supplementary File 6,
407 Figure S93). This composition was similar to the first test except for Synergistota instead of
408 Spirochaetota; Spirochaetota was still highly represented in certain samples of the second
409 tests. Methanogenic archaea belonged to *Methanothrix* and/or *Methanomicrobium*. Their
410 proportion varied significantly across treatments (Figure 2B), reaching approximately 2-3%
411 in control reactors, slightly higher proportions under NaPr conditions, and slightly lower
412 ones under NaCl conditions, compared to Ctrl. Archaea were detected in extremely low
413 proportions in the most inhibited reactors (HPr81 and HCl).
414 To identify the microbial groups specifically influenced by the treatments at a finer
415 taxonomic level, differential analysis was conducted, targeting the ASVs of archaea and
416 bacteria (Figures 4-5). Of the 276 ASVs, 145 were differentially abundant compared to Ctrl,
417 with 122 less abundant and only 26 more abundant in at least one treatment, likely
418 highlighting the limits of microbial community adaptation over the short term. Adaptation
419 was condition-specific: all treatments except NaPr20 had at least one uniquely differentially
420 abundant ASV (Supplementary File 6, Figure S94). Besides, increasing the concentration of
421 the compound of interest led to the detection of additional differentially abundant ASVs.
422 This probably reflected variable toxicity thresholds among microorganisms, with a greater
423 number of strains being affected as the concentration increased. Acidity had a stronger
424 impact than non-acidic compounds, with >100 differentially abundant ASVs under HPr81
425 or HCl versus <30 under other conditions.
426 Finally, the number of differentially abundant ASVs was negatively correlated with methane
427 production rates (R^2 = 0.9698, Supplementary File 6, Figure S95), underscoring the link
428 between AD impairment and microbial community reshaping.
429
430
431

3.6 Adaptation of microbial community to propionate (Pr^-) without acidity shift

Microbial community adaptation to Pr^- under non-acidic conditions was assessed by examining conditions NaPr20, NaPr81 and NaCl in the second tests (Figure 4).

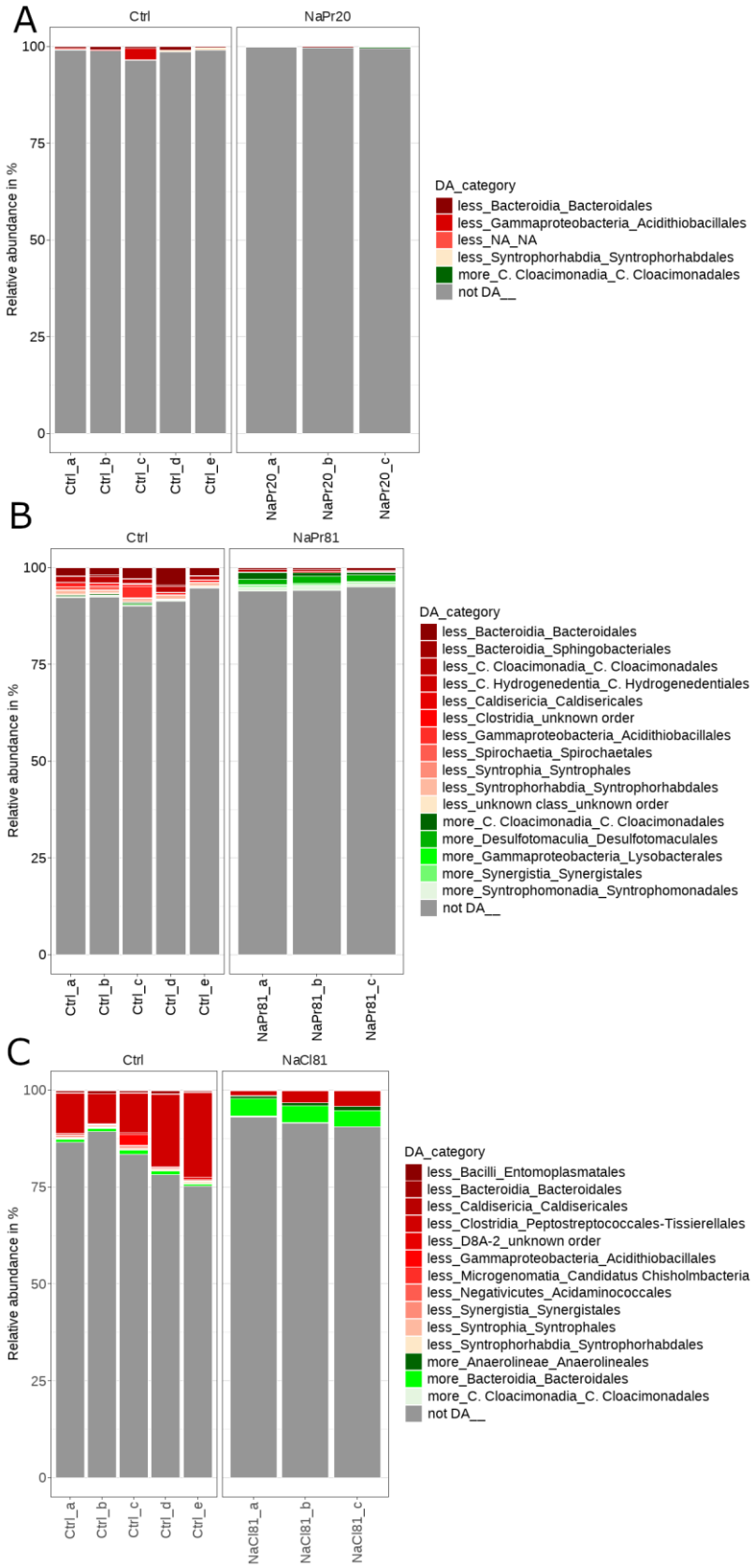

436 Figure 4. Taxonomy and relative abundance of differentially abundant ASVs identified
437 under various non-acidifying conditions, compared to Ctrl. Red indicates the ASVs that were
438 significantly less abundant in the treatment compared to Ctrl, and green, significantly more
439 abundant in the treatment compared to Ctrl. A. Comparison of NaPr20 to Ctrl. B.
440 Comparison of NaPr81 to Ctrl. C. Comparison of NaCl81 to Ctrl.
441
442
443 Under NaPr81 (Figure 4B),12 ASVs were identified as highly robust regarding adaptation
444 to Pr^-, as they were differentially abundant when comparing NaPr81 to Ctrl and NaPr81 to
445 NaCl81, but not when comparing NaCl81 to Ctrl (Supplementary File 7). Among them, the
446 most abundant ones (reaching approximately 1% in at least one sample) and those showing
447 strong reproducibility were examined more specifically. In details, the abundances of
448 ASV_2 (order Bacteroidales, family Prolixibacteraceae) and ASV_208 (order
449 Syntrophorhabdales, genus *Syntrophorhabdus*) were reduced under NaPr81, whereas
450 ASV_68 (order Lysobacterales, genus *Thermomonas*) and ASV_703 (order Synergistales,
451 family Synergistaceae) were on the contrary favored under the same condition. Members of
452 Prolixibacteraceae are facultative anaerobes, capable of fermenting certain carbohydrates
453 (Huang et al., 2014; Zhou et al., 2019). The sole isolated bacterium belonging to
454 *Syntrophorhabdus* can oxidize aromatic compounds in syntrophy with hydrogenotrophic
455 methanogens (Qiu et al., 2008). Some *Thermomonas* strains can assimilate propionate
456 (Denner et al., 2015), which may have explained their higher abundance under the high NaPr
457 concentration. According to the MIDAS database (Dueholm et al., 2024), Synergistaceae
458 bacteria ferment certain acids and amino acids but not systematically carbohydrates,
459 producing H_2 and other metabolites, sometimes propionate.
460 NaPr20 had a limited effect on both methane production and microbial community
461 composition, with only ASV_109 (Bacteroidales, Rikenellaceae, S50 wastewater-sludge

462 group) and ASV_453 (Syntrophorhabdales, *Syntrophorhabdus*) showing significant
463 differential abundance. Rikenellaceae includes obligate anaerobic microorganisms, such as
464 fermenters, according to the MIDAS database (Dueholm et al., 2024).
465
466 **3.7 Adaptation of microbial community to propionate (Pr^-) with acidity shift**
467 To decipher microbial community adaptation to Pr^- under acidic conditions, HPr20, HPr81
468 and HCl were compared to Ctrl in the second tests (Figure 5). Under HPr81, 96 ASVs were
469 significantly impaired, the most abundant being ASV_1 (order Peptostreptococcales-
470 Tissierellales, genus *Sedimentibacter*) and ASV_4 (order Anaerolineales, family
471 Anaerolineaceae, probable fermenters). Only fourteen ASVs were significantly more
472 abundant. Among them, ASV_14 and ASV_35 were both affiliated to Bacteroidales,
473 Tannerellaceae family; they reached more than 1% in average under HPr81, and were not
474 detected under Ctrl. Known Tannerellaceae members are strictly anaerobic carbohydrate
475 fermenters according to MIDAS (Dueholm et al., 2024). ASV_112 was also notable:
476 affiliated to *Lactobacillus* genus (Lactobacillales), it reached 0.74% under HPr81.
477 *Lactobacillus* corresponds to saccharolytic fermenters, facultative anaerobes, producing
478 lactate as major end-product, based on MIDAS (Dueholm et al., 2024). HPr81 and HCl
479 reactors shared specifically 64 negatively-affected ASVs (including ASV_1 and ASV_4)
480 and 10 positively-affected ASVs (including ASV_14, ASV_35 and ASV_112),
481 (Supplementary File 6, Figure S94) suggesting that under HPr81, community adaptation was
482 largely driven by the acidic pH.
483

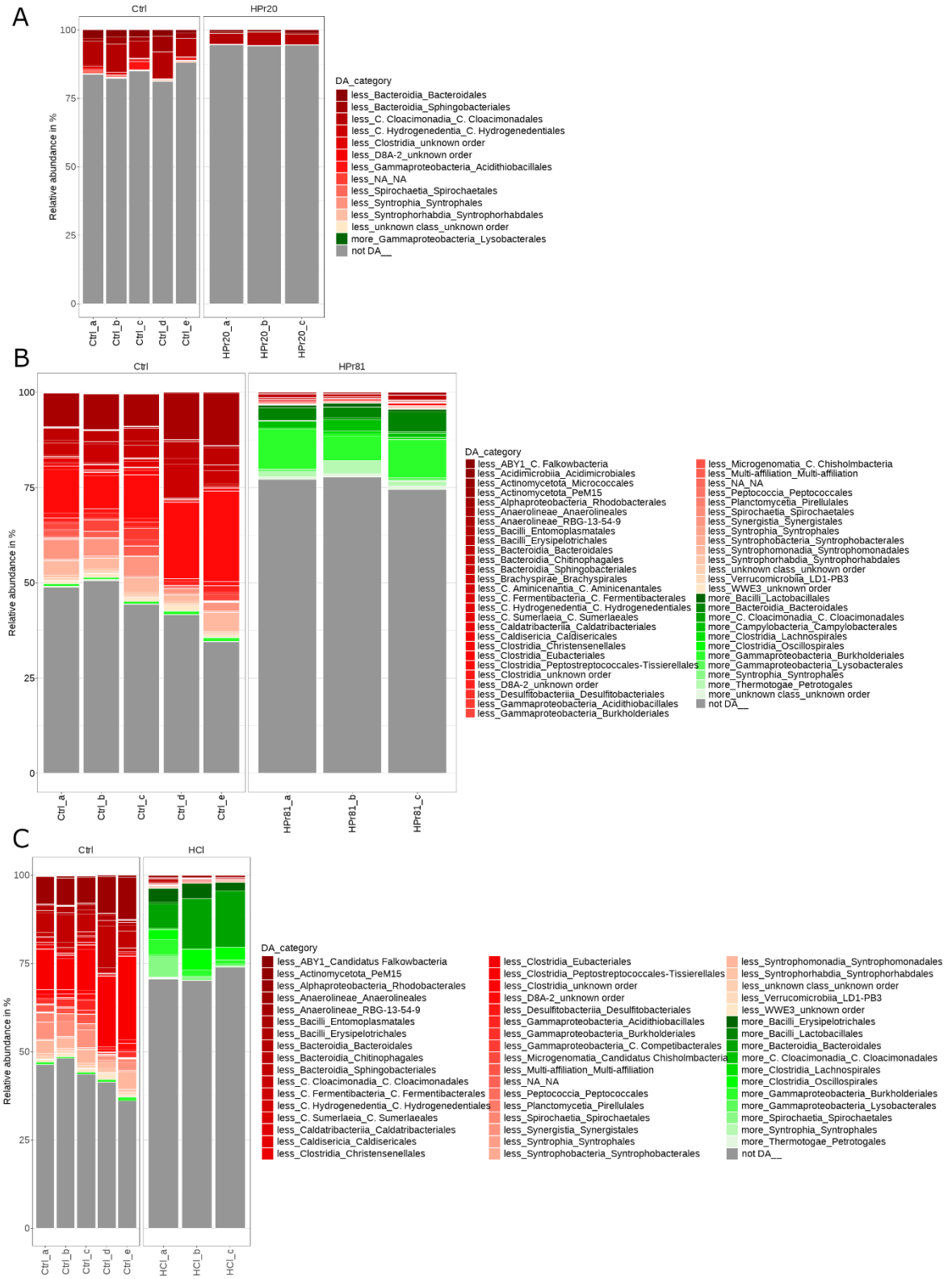

Figure 5. Taxonomy and relative abundance of differentially abundant ASVs identified under various acidifying conditions, compared to Ctrl. Red indicates the ASVs that were significantly less abundant in the treatment compared to Ctrl, and green, significantly more abundant in the treatment compared to Ctrl. A. Comparison of HPr20 to Ctrl. B. Comparison

489 of HPr81 to Ctrl. C. Comparison of HCl to Ctrl.

490

491

492 Regarding HPr20, three ASVs were notable (Figure 5C) since they both exhibited significant
493 abundances (≥ 1% in at least one treatment) and were less abundant relative to Ctrl: ASV_6
494 (order Candidatus Cloacimonadales, genus W5), ASV_16 (order Bacteroidales, family
495 Rikenellaceae, genus DMER64), and ASV_21 (order Sphingobacteriales, family ST-
496 12K33). Importantly, genus W5 is believed to correspond to syntrophic propionate oxidizing
497 bacteria (Dyksma & Gallert, 2019). Genus DMER64 is a poorly characterized, potential
498 syntrophic group (Lee et al., 2019). Although less pronounced, it is also worth noting the
499 presence of ASV_68 (order Lysobacterales, genus *Thermomonas*) in two out of three HPr20
500 reactors, while it was not detected in any of the Ctrl reactors and was also slightly but clearly
501 selected under HPr81 and HCl (Supplementary File 7).

502

503 **4. Discussion**

504 A previous study evidenced that anaerobic digesters can tolerate propionate concentrations
505 as high as 50 mM of NaPr (4,800 mg L^{-1}) (Ahring et al., 1995). More recently, it was shown
506 that 41.6 mM of NaPr (4,000 mg L^{-1}) can be fully degraded in batch reactors (Yang et al.,
507 2015). The present study is consistent with the moderate resilience of AD reactors to NaPr
508 molar concentrations up to 81 mM (7,750 mg L^{-1}), which is far higher than the threshold
509 reported for its acid form (12 mM of HPr, equivalent to 900 mg L^{-1}) (Wang et al., 2009; Han
510 et al., 2020). A recent publication (Ochoa-Bernal et al., 2025) confirms the accumulation of
511 acetate and the appearance of a shift in archaeal populations between 62.5 and 125 mM (i.e.
512 6,000 – 12,000 mg L^{-1}) of NaPr, close to the threshold of inhibition that we observed in this
513 study.

514 The maximum VFA concentration at which AD can operate depends on numerous factors.

515 On one hand, the propionate concentration is always reported relative to the media volume.
516 It does not accurately describe how propionate locally surrounds and interacts with microbial
517 cells. The ratios between inoculum, raw sludge and propionate concentrations in reactors
518 could play a key role and partially explain the differences observed among various studies
519 (e.g. 6.4 g VS L^{-1} / 54 mM in Han et al. (2020) versus 22.4 g VS L^{-1} / 81 mM in the present
520 study). On the other hand, the tolerance of AD reactors to propionic acid and its conjugated
521 base differs greatly. The present study distinguishes between pH drop and propionate effects
522 on methanogenesis inhibition, providing a unifying view.
523 The first and second tests were conducted under very similar conditions. Consistently,
524 numerous common trends regarding microbial community changes emerged when
525 comparing both tests, as summarized in Figure 6. For both HPr and NaPr, gradual shifts in
526 community composition according to the compound concentration were clearly visible,
527 highlighting distinct ranges of sensitivity and adaptation ability. Beyond this shared general
528 trend, results were different for both compounds. The rearrangements of the microbial
529 community in the presence of high NaPr concentration (NaPr81) were relatively modest in
530 terms of microbial abundance, even though the methane production rate was 40% lower than
531 in the control conditions. By contrast, under HPr81, the highly abundant fermenters
532 *Sedimentibacter* (Sedimentibacteraceae) and Anaerolineaceae were affected, as well
533 subdominant key groups such as methanogens. In addition, several microbial groups
534 specifically affected by the presence of NaPr were identified, whereas in the presence of
535 HPr, the effect appeared to be primarily linked to acidity, with many microbial groups
536 similarly affected in the presence of HCl. In both test series, the proportion of methanogenic
537 archaea decreased markedly with increasing HPr concentration, consistent with the
538 inhibition of methane production. However, the archaeal populations selected were not
539 identical across both test series. This discrepancy may reflect the use of distinct sludge
540 batches for each test series, which, despite originating from the same plant and digester, may

541 have differed slightly in composition. Moreover, since archaea operate at the terminal step
542 of the AD process, they may be particularly sensitive to the cumulative effect of small
543 variations occurring at each upstream stage.
544

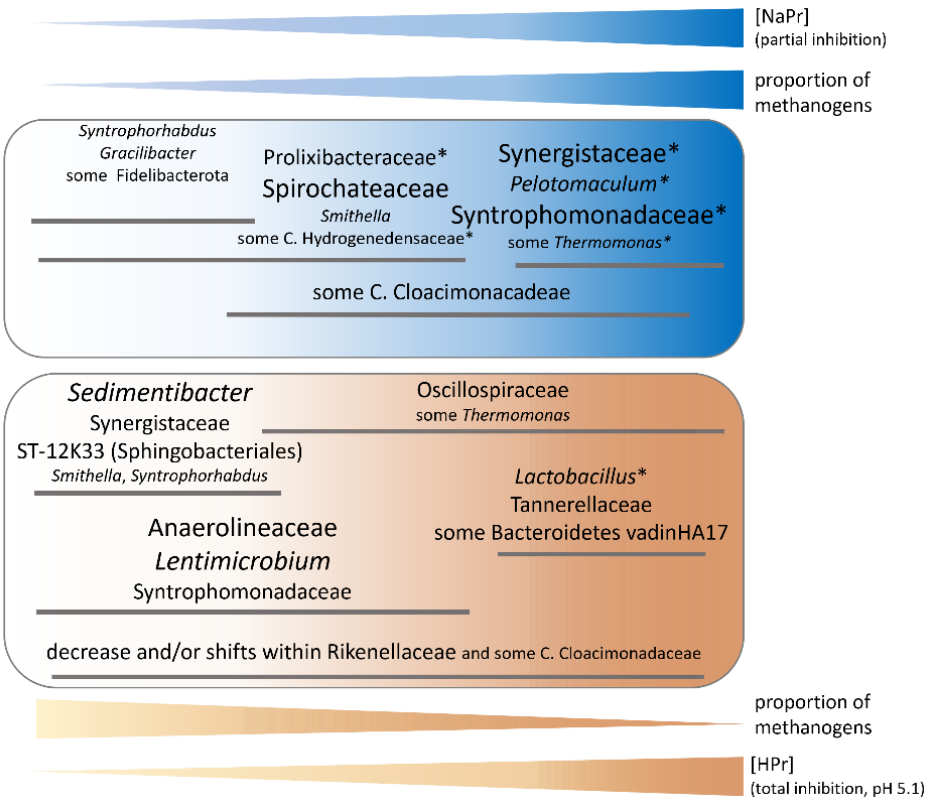

545

546 **Figure 6. Summary illustration of the adaptation of anaerobic digestion communities**
547 **exposed to various concentrations of NaPr (top) and HPr (bottom).** Asterisks indicate
548 that the effect observed was specific for the tested conditions, i.e. not observed under
549 equivalent NaCl (top) or HCl (bottom) treatment. The font size reflects the abundance of the
550 microbial groups involved.
551
552
553 Worth highlighting, in a previous study available as preprint (Camargo et al, 2023, bioRxiv),
554 acid inhibition with HPr accumulation naturally occurred during the dry co-digestion of
555 wastewater treatment sludge and horse manure, due to high organic loading; some of the
556 microorganisms negatively affected under these conditions were similar to those identified

557 in the present study. These included members of the families Sedimentibacteraceae,
558 Smithellaceae, and ST-12K33 (Sphingobacteriales), which were also inhibited by HPr in the
559 present study. *Sedimentibacter* was also negatively affected during the semi-continuous
560 mesophilic digestion of dairy manure disrupted through HPr spikes (Khafipour et al., 2020).
561 The same study documented a decrease in the abundance of *Syntrophomonas* in response to
562 HPr, which is also consistent with observations in the present study.
563 When propionic acid was added to the reactors, one might have expected antagonistic effects
564 on propionate-consuming bacteria: on the one hand, selection of these bacteria due to an
565 increase in available substrate; on the other hand, a negative effect due to acidic inhibition.
566 In the present dataset, a significant number of families possibly contained SPOB
567 (Westerholm et al., 2022). However, this activity was difficult to confirm on the basis of *16S*
568 *rDNA* sequencing alone. Indeed, the selected method yielded taxonomic assignation at the
569 genus level, and it is known that not all species within a given genus are SPOB. Based on
570 previous knowledge and on the abundance profiles, SPOB in the present study could
571 presumably belong to *Smithella* (detected under non-inhibiting conditions), *Pelotomaculum*
572 (order Desulfotomaculales, selected under high NaPr concentration), *Syntrophomonadaceae*
573 (inhibited by HPr but enriched under high NaPr concentrations), and to members of
574 Candidatus Cloacimonadaceae (showing variable responses depending on conditions)
575 (Westerholm et al., 2022).
576

577 **5. Conclusions**

578 This study provides new insights into propionic acid inhibition during anaerobic digestion
579 of municipal sewage sludge. While 20 mM HPr caused a partial inhibition of methane
580 production (22% reduction in the maximal production rate), 81 mM HPr led to complete
581 inhibition, primarily driven by the associated pH drop to 5.1 rather than by propionate ions
582 themselves — as evidenced by the fact that 81 mM NaPr only reduced the methane

583 production rate by 40% while leaving pH unaffected. Propionate ions (Pr^-) nonetheless exert
584 a secondary, concentration-dependent inhibitory effect even under neutral pH conditions.
585 Microbial community analysis revealed a substantial and gradual adaptive response,
586 insufficient to fully offset the inhibition of methane production. Community restructuring
587 was compound-specific, with HPr-treated reactors sharing numerous features with HCl
588 controls, underscoring the dominant role of acidity, while NaPr induced distinct and more
589 limited microbial shifts. Diverse functional groups were affected, including syntrophs and
590 methanogenic archaea. These findings reconcile conflicting reports in the literature by
591 distinguishing the roles of pH, undissociated HPr, and Pr^- ions, and carry direct practical
592 implications: microbial community profiling could serve as an early warning tool for process
593 imbalance detection. Further research under continuous feeding conditions could help
594 identify operational biomarkers.
595

596 **Acknowledgements**

597 This study was funded by the French research program MOCOPEE.
598

599 **Author Contributions**

600 **XL**: Conceptualization, Formal analysis, Writing – original draft, **CS**: Investigation, Formal
601 analysis, Writing – review and editing **VJ**: Data curation, Formal analysis, **AP**:
602 Conceptualization, Supervision, Writing – review and editing, **LA**: Investigation,
603 Conceptualization, Supervision, Writing – review and editing, **TR**: Conceptualization,
604 Supervision, Writing – review and editing, **S G-R**: Conceptualization, Supervision, Writing
605 – review and editing **VR**: Conceptualization, **CL**: Investigation, Conceptualization, **CB**:
606 Investigation, Writing – review and editing, **CM**: Software, Writing – review and editing,
607 **OC**: Conceptualization, Writing – review and editing, **AB**: Conceptualization, Formal
608 analysis, Writing – original draft, **C R-A**: Conceptualization, Supervision, Writing – review

and editing.

References

Ahring, B.K., Sandberg, M., Angelidaki, I. 1995. Volatile fatty acids as indicators of process imbalance in anaerobic digestors. *Applied Microbiology and Biotechnology*, **43**(3), 559-565.

Alavi-Borazjani, S.A., Capela, I., Tarelho, L.A.C. 2020. Over-acidification control strategies for enhanced biogas production from anaerobic digestion: A review. *Biomass and Bioenergy*, **143**, 105833.

Bernard, M., Rué, O., Mariadassou, M., Pascal, G. 2021. FROGS: a powerful tool to analyse the diversity of fungi with special management of internal transcribed spacers. *Briefings in Bioinformatics*, **22**(6), bbab318.

Callahan, B.J., McMurdie, P.J., Rosen, M.J., Han, A.W., Johnson, A.J.A., Holmes, S.P. 2016. DADA2: High-resolution sample inference from Illumina amplicon data. *Nature Methods*, **13**(7), 581-583.

Calusinska, M., Goux, X., Fossépré, M., Muller, E.E.L., Wilmes, P., Delfosse, P. 2018. A year of monitoring 20 mesophilic full-scale bioreactors reveals the existence of stable but different core microbiomes in bio-waste and wastewater anaerobic digestion systems. *Biotechnology for Biofuels*, **11**(1), 196.

Clark, R.H., Speece, R.E. 1971. The pH tolerance of anaerobic digestion. *Advances in Water Pollution Research*, **1**, 1-13.

Demirel, B., Yenigün, O. 2002. The Effects of Change in Volatile Fatty Acid (VFA) Composition on Methanogenic Upflow Filter Reactor (UFAF) Performance. *Environmental Technology*, **23**(10), 1179-1187.

Denner, E.B.M., Kämpfer, P., Busse, H.-J. 2015. Thermomonas. in: *Bergey's Manual of Systematics of Archaea and Bacteria*, pp. 1-6.

Dueholm, M.K.D., Andersen, K.S., Korntved, A.-K.C., Rudkjøbing, V., Alves, M., Bajón-Fernández, Y., Batstone, D., Butler, C., Cruz, M.C., Davidsson, Å., Erijman, L., Holliger, C., Koch, K., Kreuzinger, N., Lee, C., Lyberatos, G., Mutnuri, S., O'Flaherty, V., Oleskowicz-Popiel, P., Pokorna, D., Rajal, V., Recktenwald, M., Rodríguez, J., Saikaly, P.E., Tooker, N., Vierheilig, J., De Vrieze, J., Wurzbacher, C., Nielsen, P.H. 2024. MiDAS 5: Global diversity of bacteria and archaea in anaerobic digesters. *Nature Communications*, **15**(1), 5361.

Dyksma, S., Gallert, C. 2019. Candidatus Syntrophosphaera thermopropionivorans: a novel player in syntrophic propionate oxidation during anaerobic digestion. *Environmental Microbiology Reports*, **11**(4), 558-570.

EUROSTAT. Sewage Sludge Production and Disposal Available online: http://appsso.eurostat.ec.europa.eu/nui/show.do?lang=en&dataset=env_ww_spd.

Gophna, U., Konikoff, T., Nielsen, H.B. 2017. Oscillospira and related bacteria – From metagenomic species to metabolic features. *Environmental Microbiology*, **19**(3), 835-841.

Han, Y., Green, H., Tao, W. 2020. Reversibility of propionic acid inhibition to anaerobic digestion: Inhibition kinetics and microbial mechanism. *Chemosphere*, **255**, 126840.

Holliger, C., Alves, M., Andrade, D., Angelidaki, I., Astals, S., Baier, U., Bougrier, C., Buffière, P., Carballa, M., de Wilde, V., Ebertseder, F., Fernández, B., Ficara, E., Fotidis, I., Frigon, J.-C., de Laclos, H.F., Ghasimi, D.S.M., Hack, G., Hartel, M., Heerenklage, J., Horvath, I.S., Jenicek, P., Koch, K., Krautwald, J., Lizasoain, J., Liu, J., Mosberger, L., Nistor, M., Oechsner, H., Oliveira, J.V., Paterson, M., Pauss, A., Pommier, S., Porqueddu, I., Raposo, F., Ribeiro, T., Rüsch Pfund, F., Strömberg,

S., Torrijos, M., van Eekert, M., van Lier, J., Wedwitschka, H., Wierinck, I. 2016. Towards a standardization of biomethane potential tests. *Water Science and Technology*, **74**(11), 2515-2522.

Huang, X.-F., Liu, Y.J., Dong, J.-D., Qu, L.-Y., Zhang, Y.-Y., Wang, F.-Z., Tian, X.-P., Zhang, S. 2014. Mangrovibacterium diazotrophicum gen. nov., sp. nov., a nitrogen-fixing bacterium isolated from a mangrove sediment, and proposal of Prolixibacteraceae fam. nov. *International Journal of Systematic and Evolutionary Microbiology*, **64**(Pt_3), 875-881.

Imachi, H., Sakai, S., Kubota, T., Miyazaki, M., Saito, Y., Takai, K. 2016. Sedimentibacter acidaminivorans sp. nov., an anaerobic, amino-acid-utilizing bacterium isolated from marine subsurface sediment. *International Journal of Systematic and Evolutionary Microbiology*, **66**(3), 1293-1300.

Jiang, C., Peces, M., Andersen, M.H., Kucheryavskiy, S., Nierychlo, M., Yashiro, E., Andersen, K.S., Kirkegaard, R.H., Hao, L., Høgh, J., Hansen, A.A., Dueholm, M.S., Nielsen, P.H. 2021. Characterizing the growing microorganisms at species level in 46 anaerobic digesters at Danish wastewater treatment plants: A six-year survey on microbial community structure and key drivers. *Water Research*, **193**, 116871.

Jiang, Y., Dennehy, C., Lawlor, P.G., Hu, Z., McCabe, M., Cormican, P., Zhan, X., Gardiner, G.E. 2018. Inhibition of volatile fatty acids on methane production kinetics during dry co-digestion of food waste and pig manure. *Waste Management*, **79**, 302-311.

Jouan-Rimbaud Bouveresse, D., Rutledge, D.N. 2024. A synthetic review of some recent extensions of ComDim. *Journal of Chemometrics*, **38**(5), e3454.

Khafipour, A., Jordaan, E.M., Flores-Orozco, D., Khafipour, E., Levin, D.B., Sparling, R., Cicek, N. 2020. Response of Microbial Community to Induced Failure of Anaerobic Digesters Through Overloading With Propionic Acid Followed by Process Recovery. *Frontiers in Bioengineering and Biotechnology*, **8**.

Lee, J., Koo, T., Yulisa, A., Hwang, S. 2019. Magnetite as an enhancer in methanogenic degradation of volatile fatty acids under ammonia-stressed condition. *Journal of Environmental Management*, **241**, 418-426.

Li, Y., Zhang, Y., Sun, Y., Wu, S., Kong, X., Yuan, Z., Dong, R. 2017. The performance efficiency of bioaugmentation to prevent anaerobic digestion failure from ammonia and propionate inhibition. *Bioresource Technology*, **231**, 94-100.

Liu, Y., Whitman, W.B. 2008. Metabolic, Phylogenetic, and Ecological Diversity of the Methanogenic Archaea. *Annals of the New York Academy of Sciences*, **1125**(1), 171-189.

Love, M.I., Huber, W., Anders, S. 2014. Moderated estimation of fold change and dispersion for RNA-seq data with DESeq2. *Genome Biology*, **15**(12), 550.

McMurdie, P.J., Holmes, S. 2013. phyloseq: An R Package for Reproducible Interactive Analysis and Graphics of Microbiome Census Data. *PLOS ONE*, **8**(4), e61217.

Ochoa-Bernal, T.G., Huber, D.H., Espinosa-Solares, T. 2025. The progressive shift in anaerobic digestion communities under extreme propionate levels led to a redundant microbiome capable of producing methane. *Journal of Environmental Management*, **395**, 127698.

Poirier, S., Bize, A., Bureau, C., Bouchez, T., Chapleur, O. 2016. Community shifts within anaerobic digestion microbiota facing phenol inhibition: Towards early warning microbial indicators? *Water Research*, **100**, 296-305.

Puig-Castellví, F., Cardona, L., Jouan-Rimbaud Bouveresse, D., Cordella, C.B.Y., Mazéas, L., Rutledge, D.N., Chapleur, O. 2020. Assessment of the microbial interplay during anaerobic co-digestion of wastewater sludge using common components analysis. *PLOS ONE*, **15**(5), e0232324.

Qiao, W., Takayanagi, K., Niu, Q., Shofie, M., Li, Y.Y. 2013. Long-term stability of thermophilic co-digestion submerged anaerobic membrane reactor encountering

high organic loading rate, persistent propionate and detectable hydrogen in biogas. *Bioresource Technology*, **149**, 92-102.

Qiu, Y.-L., Hanada, S., Ohashi, A., Harada, H., Kamagata, Y., Sekiguchi, Y. 2008. Syntrophorhabdus aromaticivorans gen. nov., sp. nov., the First Cultured Anaerobe Capable of Degrading Phenol to Acetate in Obligate Syntrophic Associations with a Hydrogenotrophic Methanogen. *Applied and Environmental Microbiology*, **74**(7), 2051-2058.

Roe Andrew, J., McLaggan, D., Davidson, I., O'Byrne, C., Booth Ian, R. 1998. Perturbation of Anion Balance during Inhibition of Growth of Escherichia coli by Weak Acids. *Journal of Bacteriology*, **180**(4), 767-772.

Sakai, S., Ehara, M., Tseng, I.-C., Yamaguchi, T., Bräuer, S.L., Cadillo-Quiroz, H., Zinder, S.H., Imachi, H. 2012. Methanolinea mesophila sp. nov., a hydrogenotrophic methanogen isolated from rice field soil, and proposal of the archaeal family Methanoregulaceae fam. nov. within the order Methanomicrobiales. *International Journal of Systematic and Evolutionary Microbiology*, **62**(Pt_6), 1389-1395.

Sawyer, C.N., Howard, F.S., Pershe, E.R. 1954. Scientific Basis for Liming of Digesters. *Sewage and Industrial Wastes*, **26**(8), 935-944.

Scarlat, N., Dallemand, J.-F., Fahl, F. 2018. Biogas: Developments and perspectives in Europe. *Renewable Energy*, **129**, 457-472.

Sekiguchi, Y. 2015. Syntrophomonas. in: *Bergey's Manual of Systematics of Archaea and Bacteria*, pp. 1-11.

Sikora, A., Detman, A., Chojnacka, A., Błaszczyk, M.K. 2017. Anaerobic digestion: I. A common process ensuring energy flow and the circulation of matter in ecosystems. II. A tool for the production of gaseous biofuels. *Fermentation processes*, **14**, 271.

Sousa, D.Z., Smidt, H., Alves, M.M., Stams, A.J.M. 2007. Syntrophomonas zehnderi sp. nov., an anaerobe that degrades long-chain fatty acids in co-culture with Methanobacterium formicicum. *International Journal of Systematic and Evolutionary Microbiology*, **57**(3), 609-615.

Team, R.C. 2021. A language and environment for statistical computing. *(No Title)*.

Wang, Y., Zhang, Y., Wang, J., Meng, L. 2009. Effects of volatile fatty acid concentrations on methane yield and methanogenic bacteria. *Biomass and Bioenergy*, **33**(5), 848-853.

Westerholm, M., Calusinska, M., Dolfing, J. 2022. Syntrophic propionate-oxidizing bacteria in methanogenic systems. *FEMS Microbiology Reviews*, **46**(2), fuab057.

Yang, Y., Chen, Q., Guo, J., Hu, Z. 2015. Kinetics and methane gas yields of selected C1 to C5 organic acids in anaerobic digestion. *Water Research*, **87**, 112-118.

Zhou, L.-Y., Yu, Z.-L., Xu, W., Mu, D.-S., Du, Z.-J. 2019. Maribellus luteus gen. nov., sp. nov., a marine bacterium in the family Prolixibacteraceae isolated from coastal seawater. *International Journal of Systematic and Evolutionary Microbiology*, **69**(8), 2388-2394.